

Liquid metal MHD research at KIT: Fundamental phenomena and flows in complex blanket geometries

L. Bühler^{*}, H.-J. Brinkmann, C. Courtessole, V. Klüber, C. Koehly, B. Lyu, C. Mistrangelo, J. Roth

Karlsruhe Institute of Technology (KIT), P.O. Box 3640, 76021 Karlsruhe, Germany

ARTICLE INFO

Keywords:

Magnetohydrodynamics (MHD)
Liquid metal breeder blankets
MHD pressure drop
Model experiments
Benchmark data

ABSTRACT

The present paper gives an overview of liquid metal research activities performed in recent years at the Karlsruhe Institute of Technology (KIT). The work is motivated by applications in liquid metal blankets for a DEMO fusion reactor where lead lithium (PbLi), which serves as a neutron multiplier and tritium breeder, interacts with the plasma-confining magnetic field as it flows in the blanket covering the inner walls of the reactor. Liquid metal magnetohydrodynamic (MHD) research at KIT supports blanket design activities through theoretical and experimental investigations. Predictive computational tools are developed and validated by empirical data obtained for fundamental problems, such as flows in non-uniform magnetic fields or magneto-convective heat transfer from submerged obstacles. In addition, technological developments like pressure drop reduction by insulating flow channel inserts are pursued both theoretically and experimentally. Two complementary experimental facilities (MEKKA and MaPLE) provide a unique and versatile platform for MHD investigations at fusion relevant parameters. Using NaK as a model fluid in MEKKA allows experiments to be conducted at high Hartmann numbers in large complex geometries, such as scaled blanket mock-ups of ITER test blanket modules. For magneto-convection and heat transfer studies, MaPLE is well suited since it enables experiments with the prototypical fluid PbLi in test sections inclined at various orientations with respect to gravity. Some recent results have been selected to illustrate the broad spectrum of MHD activities at KIT.

1. Introduction

Lead-lithium (PbLi) is foreseen to be used as breeder material for tritium production and heat transfer medium for power extraction in fusion breeder blankets. In the European concept of a water-cooled lead-lithium blanket, the volumetric heat released by neutron energy deposition is removed by water flowing at high pressure in channels embedded into the blanket walls and in cooling pipes immersed in the eutectic alloy. The liquid metal is circulated via manifolds and pipes to ancillary systems for tritium extraction and purification. The PbLi flow is altered by buoyancy due to temperature gradients occurring between the volumetrically heated bulk of liquid metal and water-cooled surfaces. Furthermore, the motion of the electrically conducting fluid within the plasma-confining magnetic field is affected by electromagnetic Lorentz forces that arise from flow-induced electric currents and cause large pressure drop and peculiar velocity profiles. Moreover, leakage currents across electrically conducting walls result in electromagnetic coupling of neighboring fluid regions. The dominating influence of magnetohydrodynamics (MHD) on the liquid metal flow impacts heat and mass transfer. Therefore, the development of reliable liquid metal blankets requires a deep understanding of complex coupled

multi-physics phenomena and the advancement of validated predictive tools.

The present paper gives an overview of recent research activities at the Karlsruhe Institute of Technology (KIT) in the field of liquid metal magnetohydrodynamics, magneto - convection and heat transfer, and technological developments for applications in liquid metal blankets. The MHD research at KIT exploits the synergies between theoretical analysis, computational modeling, and experimental activities offered by the unique MHD platform consisting of the MEKKA and MaPLE facilities.

2. Liquid metal magnetohydrodynamics

Liquid metal flows in strong magnetic fields are governed by a balance of momentum, where inertia force balances pressure, viscous, and electromagnetic Lorentz forces,

$$\frac{1}{N} (\partial_t \mathbf{u} + (\mathbf{u} \cdot \nabla) \mathbf{u}) = -\nabla p + \frac{1}{Ha^2} \nabla^2 \mathbf{u} + \mathbf{j} \times \mathbf{B}. \quad (1)$$

^{*} Corresponding author.

E-mail address: leo.buehler@kit.edu (L. Bühler).

The current density \mathbf{j} that determines the strength of the Lorentz force $\mathbf{j} \times \mathbf{B}$ results from Ohm's law

$$\mathbf{j} = -\nabla\phi + \mathbf{u} \times \mathbf{B}.$$

Currents are driven by the gradient of an electric field ϕ and a flow-induced electric field $\mathbf{u} \times \mathbf{B}$. The flow is assumed incompressible with $\nabla \cdot \mathbf{u} = 0$ and charge conservation requires $\nabla \cdot \mathbf{j} = 0$. In the above nondimensional notation, $\mathbf{u}, \mathbf{B}, \mathbf{j}, p$, and ϕ denote fluid velocity, magnetic field, current density, pressure, and electric potential, scaled by a characteristic quantities u_0 , B_0 , $\sigma u_0 B_0$, $\sigma u_0 L B_0^2$, and $u_0 B_0 L$, respectively. With length scale L , mass density ρ , kinematic viscosity ν and electric conductivity σ , the nondimensional parameters governing the flow, i.e. the interaction parameter N and the Hartmann number Ha become

$$N = \frac{\sigma L B_0^2}{\rho u_0} \text{ and } Ha = L B_0 \sqrt{\frac{\sigma}{\rho \nu}},$$

where N and Ha^2 quantify the ratios electromagnetic/ inertia forces and electromagnetic/ viscous forces, respectively. The hydrodynamic Reynolds number is obtained as $Re = Ha^2/N$. For applications in fusion blankets, the Lorentz force is dominant since $N \approx 10^3 \div 2 \cdot 10^5$ and $Ha \approx 6 \cdot 10^3 \div 3 \cdot 10^4$ [1]. This may lead to very high pressure drop, strong impact on velocity distribution and often to suppression of turbulence and deterioration of heat transfer.

For non-isothermal problems with strong buoyancy effects we have to consider in addition the heat equation to determine temperature, and Eq. (1) has to be complemented by the buoyancy term with the Grashof number

$$Gr = \frac{g \beta \Delta T L^3}{\nu^2}$$

as an additional parameter quantifying the intensity of buoyant forcing. Here g stands for gravity, β denotes the volumetric expansion coefficient and ΔT is a typical temperature difference.

3. MHD research at KIT

MHD research performed at KIT supports design activities for DEMO blankets or for test blanket modules (TBM) to be tested in ITER through numerical simulations, asymptotic analyses, and experimental studies [2–7]. Numerical simulations rely on finite volume techniques with a current-conservative formulation [8] based on OpenFOAM. Asymptotic analyses exploit the ideas of Kulikovskii [9] using boundary fitted coordinates [10]. The theoretical work is complemented and assisted by experimental data for validation purposes. Reciprocally, numerical results may help interpret experimental data and shed light on interesting flow-internal details, which might otherwise remain hidden inside the opaque liquid metal.

The experimental research at KIT is performed on an MHD platform that includes two unique and complementary facilities (MEKKA and MaPLE) for addressing the MHD challenges of liquid metal breeding blankets. They allow for investigations at fusion-relevant parameters, experiments in complex geometries and large volumes, and studies of combined MHD and buoyancy effects. Experiments can either be performed in fundamental geometries to improve the understanding of coupled multi-physics phenomena and expand the database for code benchmarking, or support technological developments. For instance, experimental campaigns have been carried out to test new measuring techniques [11], to assess pressure drop reduction by insulating flow channel inserts (FCI) [12], or to validate design concepts with scaled mock-up tests of entire blanket modules [13–15].

MEKKA (Magnetohydrodynamische Experimente mit Natrium Kalium Karlsruhe) consists of a liquid metal loop (surrogate fluid NaK, inventory 200 l, pump 9 bar, 25 m³/h, possibility for using up to 30 pressure taps, 600 potential sensors) and a large dipole magnet (2.1T, uniform with deviations smaller than 1% in a volume of 800 × 483 ×

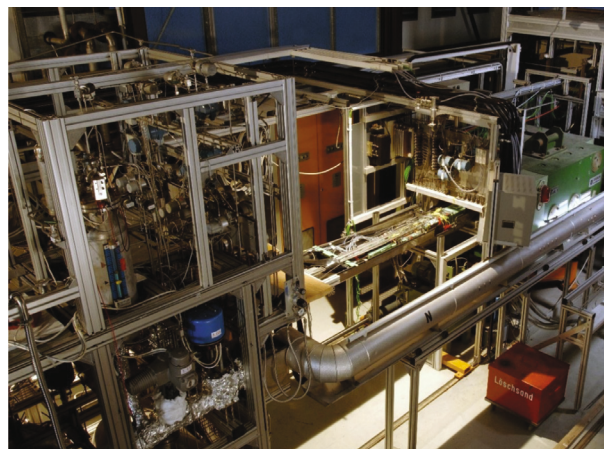


Fig. 1. View on a part of the MEKKA liquid metal loop (left) and a test section in front of the magnet (right).

168 mm³) [16]. A view of the MEKKA facility is shown in Fig. 1 with the liquid metal circuit (left) and a test-section positioned in front of the magnet (green cube on the right). Apart from the drawback of using an alkali alloy that is very reactive in contact with air or water, and therefore that has to be handled with care and kept permanently under inert gas atmosphere, MEKKA offers a variety of advantages for MHD experiments. For instance, the physical properties of NaK, with higher values of the ratio (σ/ρ) compared to PbLi, allow approaching high values of Ha and N that are relevant for fusion applications with available magnetic fields in the laboratory. Moreover, MHD experiments can be performed at constant ambient temperature, which simplifies experimental work. It also minimizes thermoelectric perturbations, which leads to more accurate electric potential measurements.

MaPLE (Magnetohydrodynamic PbLi Experiments) was built and first operated at UCLA. In collaboration with EUROfusion, the facility was later upgraded to enable investigations of combined MHD and buoyancy effects before being relocated to KIT. Like MEKKA, the facility consists of a liquid metal circulation loop associated with a large dipole magnet. The liquid metal loop uses the prototypical eutectic alloy PbLi (inventory 70 l, pump 6 bar, 7.2 m³/h) and is operated at a nominal temperature above 300 °C. The main feature of MaPLE is that its magnet is installed on a hydraulic positioning frame that allows us to work with various orientations of the magnetic volume (1.8T in 800×150×150 mm³ [17]) with respect to gravity (Fig. 2). The latter point is critical for experiments where MHD heat transfer with buoyancy effects are investigated.

4. Some illustrative results

In the following, we highlight some results of MHD flow studies, which have been recently obtained at KIT. The purpose is to give an overview showing the broad scope of activities ranging from fundamental research on basic phenomena to applied engineering problems. Therefore, details are omitted in this brief presentation, but interested readers may find more information in original publications on these topics for which references are provided.

4.1. A fundamental problem in MHD pipe flow

Magnetohydrodynamic flow in a straight electrically conducting pipe and in a spatially varying magnetic is a fundamental problem that has attracted the interest of researchers since the work of Reed & Picologlou (1989) [18,19]. In spite of the geometric simplicity, the flow exhibits complex current paths and pronounced 3D MHD effects, such that numerical simulations for large Hartmann numbers ($Ha > 1000$)



Fig. 2. Positioning frame with MaPLE magnet.

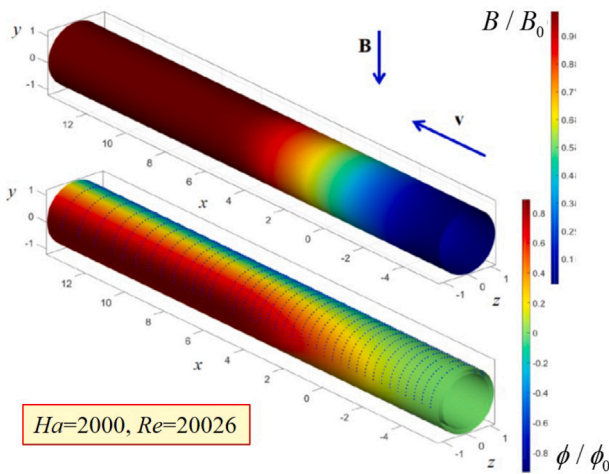


Fig. 3. Contours of measured magnetic field component $B_y(x)/B_0$ and potential scaled by $\phi_0 = u_0 L B_0$ on the pipe surface (dots denote positions of potential sensors).

are quite challenging. Experimental results, as those presented in the latter references, have been proposed and widely used for validation of predictive tools [20,21]. In this respect, the experiments performed at KIT [22] should be regarded as complementary to the work of Reed & Picologlou, since in MEKKA the magnetic field B increases almost linearly over a long distance along the pipe axis. Moreover, measurements of surface potential have been performed with a quite dense population of electrodes on the circumference of the pipe and at many axial positions. Results for $B(x)$ and surface potential of a typical measurement are shown in Fig. 3 for $Ha = 2000$ and $Re = 20026$.

Electric potential data is of interest since it is possible to derive from the measurements an approximation of velocity in the entire domain as $u(y, z) \approx B_y^{-1} \partial \phi / \partial z$, after the surface data is “projected” onto the fluid-wall interface [23]. One result is shown in Fig. 4. The experimental data (a) reveals higher velocity close to the sides and reduced flow in the center of the pipe when the magnetic field starts increasing e.g. at position (II). These high velocity jets have been confirmed by numerical simulations that show the transition from a turbulent hydrodynamic inflow (I) to a fully developed laminar MHD flow (III) [5,24]. A quite good quantitative comparison of experimental and numerical results is shown in the latter reference.

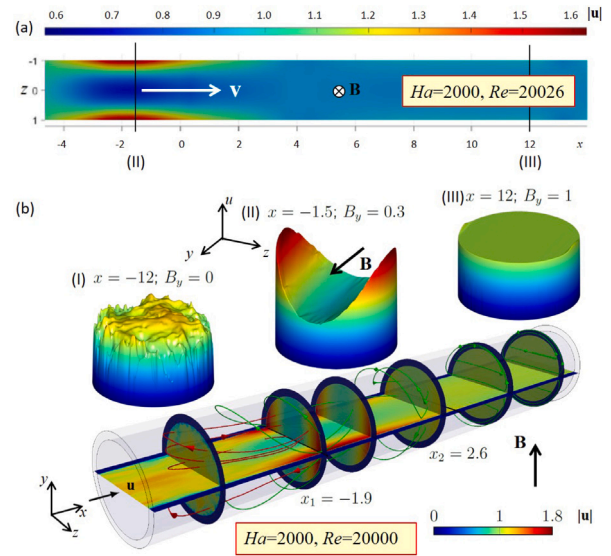


Fig. 4. Contours of velocity reconstructed from experimental data (a), and numerically obtained velocity profiles (b) of the turbulent inflow far upstream (I), at the rising magnetic field (II), and for fully developed MHD flow (III). The figure shows in addition some complex current paths. The figure has been adapted from [5,23].

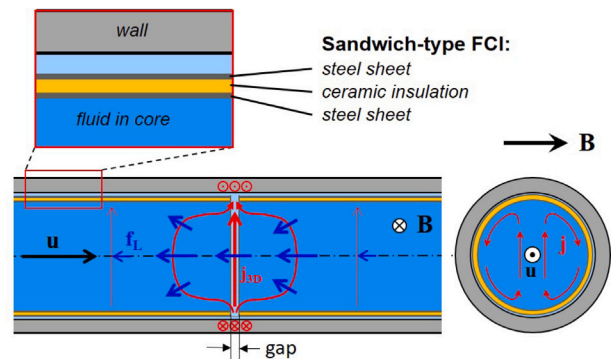


Fig. 5. Sketch showing 3D currents and Lorentz forces near a gap at the junction between two sandwich-type FCIs.

4.2. An applied engineering problem in MHD pipe flow

Highest currents and pressure drop are observed when duct or pipe walls are highly electrically conducting ($\partial_{x,p} \approx 14$ bar/m for PbLi at 0.1 m/s, 4T). Instead, if walls are insulating, the electric shortcut along the wall is interrupted and the pressure gradient can be reduced to only a few mbar/m. For reasonable MHD performance, electrical insulation of the wall is therefore a key feature. However, since structural walls are fabricated from electrically conducting steel and because the long-term integrity of thin insulating coatings in contact with PbLi has not yet been proven at high temperatures and under irradiation, Malang (1987) [25] proposed to place so-called insulating flow channel inserts (FCI) into the ducts. In the latter reference, sandwich-type FCIs are proposed where the electrically insulating ceramics is protected from a direct PbLi contact by thin sheets of steel. For applications in long ducts, or complex geometries, it is likely that several FCIs have to be employed, thus leaving small non-insulated local gaps along the flow path at junctions between FCIs across which some currents may leak into the duct walls as sketched in Fig. 5. Such perturbations in the current field result in additional Lorentz forces that cause significant local 3D MHD phenomena.

For the present problem, numerical simulations have been performed taking into account the thick conducting pipe wall and the

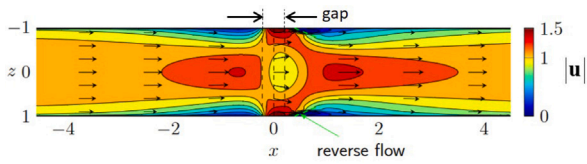


Fig. 6. Contours of velocity upstream and downstream of a gap between two FCIs for $Ha = 2000$ and $Re = 20000$ [5].

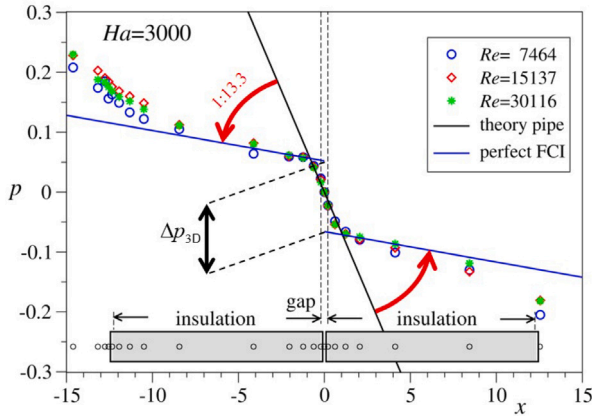


Fig. 7. Measured pressure distribution $p(x, Re)$ near a junction between two FCIs. Results are compared to theoretical predictions for fully developed pipe flow without FCI (black line) and for a fully established flow in perfect FCIs (blue lines).

complete FCI geometry, namely the ceramic insulation and thin protecting sheets. The flow in the core and in the thin annular space between the FCI and the wall was computed. Details such as additional pressure drop or even locally reversed flow in the annular region can be found in [5]. While the highest currents and Lorentz forces are observed in the vicinity of the gap, the disturbance of the flow may extend over long distances upstream and downstream of the gap as shown for instance by velocity contours in Fig. 6.

This numerical work was motivated by an experimental campaign carried out in the MEKKA facility where two FCIs developed at KIT [26] were positioned in a thick-walled pipe along which pressure and electric potential were recorded. One result showing the pressure distribution along the axial coordinate x is displayed in Fig. 7. We observe in both FCIs a strong pressure gradient reduction by a factor of more than 13 compared to that in the pipe without FCI. Near the gap, 3D effects increase locally the pressure drop by Δp_{3D} that is independent of Re in the present scaling and parameter range. Deviations from the ideal FCI predictions far upstream and downstream ($|x| \gtrsim 10$) are due to 3D entrance and exit effects [27].

The experiments can be considered as a proof of principle for the new fabrication procedure proposed by KIT for FCIs of circular shape and they reveal and confirm all phenomena found by numerical simulations.

4.3. Fundamental research related to WCLL blankets

A recent review article by Zikanov and coauthors (2021) [28] shows that a reasonable database on forced or mixed magneto-convective heat transfer in pipes and ducts already exists in addition to extensive studies of the classical Rayleigh–Bénard problem [29] or convection in vertical slots [30]. However, MHD heat transfer from submerged obstacles, such as cooling pipes in WCLL blankets, has been addressed only in a few publications. In order to study in detail buoyant MHD heat transfer from cylindrical obstacles, the problem has been reduced to the fundamental case shown in Fig. 8, where two differentially heated

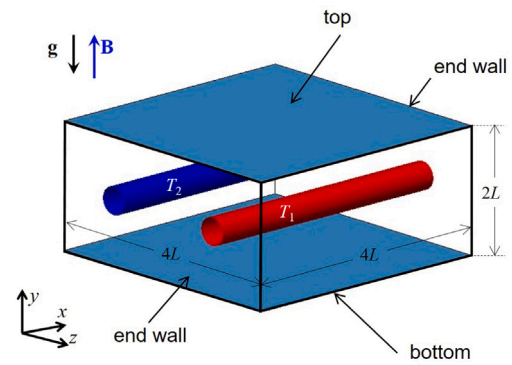


Fig. 8. Definition of a fundamental heat transfer problem with two differentially heated cylinders.

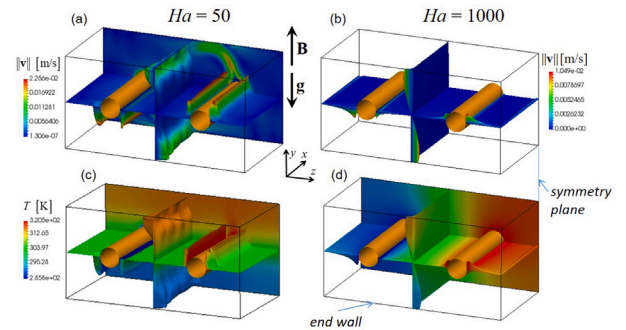


Fig. 9. Magneto convection at $Gr = 5 \cdot 10^7$, $Ha = 50$ (a, c) and $Ha = 1000$ (b, d). Velocity field (a, b) and temperature (c, d).

cylinders are immersed in the liquid metal contained in an adiabatic box [31]. All surfaces in contact with the surrogate fluid GaInSn are electrically insulating. The buoyant motion results from temperature gradients in the fluid that occur due to heat transfer between the two cylinders kept at constant temperatures $T_{1,2} = T_0 \pm \Delta T$, where T_0 is the reference temperature.

Numerical results for velocity and temperature of magneto buoyant flow for $Gr = 5 \cdot 10^7$ at weak ($Ha = 50$) and strong ($Ha = 1000$) magnetic fields are shown in Fig. 9. For moderate values of Ha , the fluid rises upwards in thin layers around the hot pipe, moves along the top wall to the other side where it falls down in thin layers around the cold pipe. As a result of the strong convective heat flux and turbulent mixing, the temperature field becomes stratified with preferentially horizontal isotherms and hot fluid on top and cold fluid at the bottom in most of the cavity. With increasing magnetic field, the fluid velocity reduces progressively, and, e.g. for $Ha = 1000$, some small velocity remains only in thin boundary layers along the end walls, while the fluid core is practically at rest. As a consequence, the convective heat transfer becomes negligible and isotherms in the middle of the cavity ($z = 0$) at some distance from the end walls become aligned vertically. More details can be found in [32].

Isotherms for the two extreme cases, i.e. for strong convection and for pure heat conduction, are plotted in Fig. 10 for illustration.

These numerical results are supported by experimental data used, for instance, to estimate the intensity of heat transfer expressed in terms of the nondimensional Nusselt number $Nu = hL/k$. Here k is the thermal conductivity of the liquid metal and h denotes the heat transfer coefficient that determines the average surface heat flux on the pipes, $q'' = \pm h \Delta T$. The latter quantity is obtained from an energy balance of the total injected and extracted thermal power at the cylinders, divided by the interface area in contact with the liquid metal (for more details see e.g. [33]). Fig. 11 shows Nu for a wide range of Gr and Ha . It

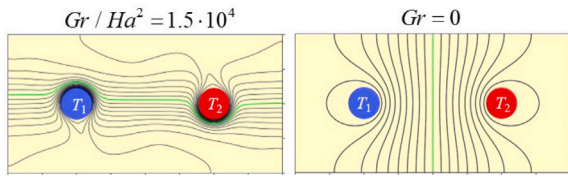


Fig. 10. Isotherms in the middle of the cavity at $x = 0$ for strong convection (left) and heat conduction (right). The green lines denote $T = T_0$, the distance between two isotherms is $0.1 \Delta T$.

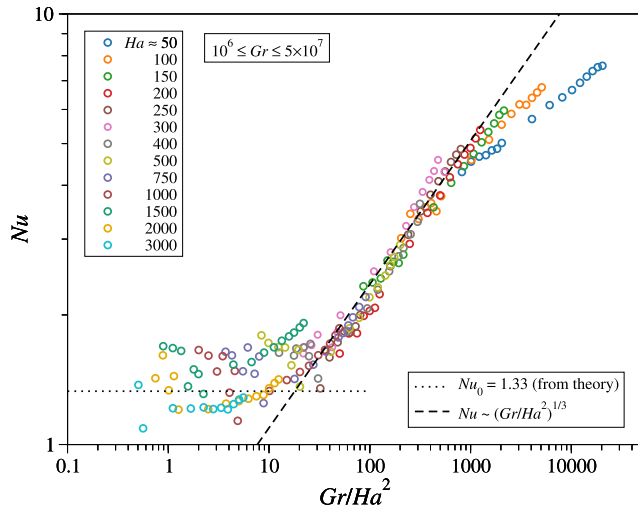


Fig. 11. Nusselt numbers for flows at $10^6 \leq Gr \leq 5 \cdot 10^7$ and $50 \leq Ha \leq 3000$ obtained in experiments.

is found that in the considered parametric range, results depend on a combination of both control parameters as Gr/Ha^2 which represents the ratio buoyancy/electromagnetic forces. For $Gr/Ha^2 \lesssim 10$, the Nusselt number tends to a constant value in reasonable agreement with theoretical predictions for heat conduction when all flow is suppressed by magnetic damping. In a transition region, $20 < Gr/Ha^2 < 1000$, the heat transfer increases due to stronger convective contributions, and for $Gr/Ha^2 \gtrsim 1000$, the flow is probably time-dependent or somehow turbulent (even if there might be a significant difference compared to hydrodynamic flows). It should be noted that measurements in the low Gr regime are quite challenging since very small temperature differences have to be resolved [33].

4.4. Applied studies supporting WCLL TBM design activities

To support the ITER WCLL TBM development, a scaled mock-up consisting of one column of breeder units fed and drained by manifolds has been designed and manufactured at KIT [34] for liquid metal MHD experiments in MEKKA. The mock-up shown in Fig. 12 consists of 8 breeder units (BUs) with baffle plates stacked along the poloidal direction, feeding (blue) and draining (red) manifolds with openings into the BUs, and dummy cylinders mimicking water-cooled pipes as solid obstacles for the flow. When entering the test-section, the liquid metal flow passes pressure tap Pin in the circular pipe, and 9 taps FM1 \div FM9 along the feeding manifold. Pressure taps BU1 \div BU8 are located on the first wall at the poloidal positions of the baffle plates, where the flow turns from radial to poloidal to radial direction. The fluid collected in the draining manifold passes taps DM1 \div DM9 before it reaches Pout in the outlet pipe.

The distribution of measured pressure as a function of the coordinate s that increases along typical flow paths is shown in Fig. 13, where results are scaled by $p_M = \sigma u_M L_M B_0^2$ with the mean velocity

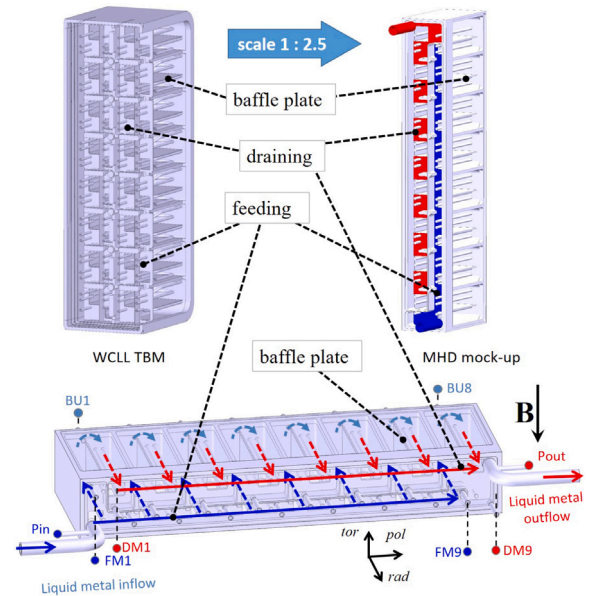


Fig. 12. Design of a scaled MHD mock-up (top-right and bottom) with one column of breeder units derived from the ITER WCLL TBM (top-left). Sketch of typical flow paths (bottom).

in manifolds $u_M = Q/A_M$ defined by the total volumetric flow rate Q and cross-section of both manifolds A_M (for more details see [15]). High pressure drop contributions are observed when the liquid metal expands from the pipe into the feeding manifold (Pin – FM1), when it moves along feeding (FM1 – FM9) and draining (DM1 – DM9) manifolds, and at the contraction from the draining manifold into the exit pipe (DM9 – Pout). Although pressure drops in the BUs are comparatively small, we observe larger values in BU1 and BU8 (FM1 – DM1 and FM9 – DM9) than in other BUs. This is caused by the fact, that a large fraction of flow swaps via BU1 (and BU2) from the feeding to the larger draining manifold. The flow across BU3 \div BU6 is quite small and the remaining flow in the feeding manifold is transferred via BU7 and BU8 into the draining duct. This results in a flow imbalance between central and lateral BUs and yields a non-symmetric distribution along the poloidal direction caused by different cross-sections of feeding and draining ducts. Similar results had been predicted by theoretical analyses [6,7] and numerical simulations [4]. The complete experimental campaign (not shown here) provides in a systematic way a number of experimental data sets for different Ha and Re from which one may conclude that inertia effects are likely negligible for ITER parameters [15].

Finally, we may conclude that the total liquid metal pressure drop for the ITER TBM remains acceptable due to the very small velocities foreseen in BUs. A major concern for the current design is the flow imbalance among BUs. This problem may be solved by modifying the geometry of feeding and draining manifolds, that should be optimized for achieving uniform flow in all BUs, as proposed e.g. in [7].

While buoyancy effects might affect flow patterns in single BUs where the velocity of the forced flow is very small, it is not expected that thermal convection has a major impact on the flow in manifolds since all heat deposited in BUs is removed by efficient water cooling before the liquid metal reaches the exit manifold. In the present TBM blanket concept the entrance and exit PbLi temperatures are designed both near 295 °C, i.e. the manifolds are preferentially isothermal so that buoyancy is not expected to have a significant impact on the liquid metal flows in manifolds.

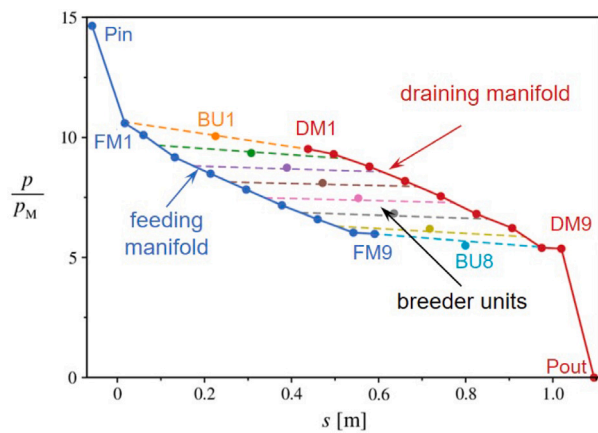


Fig. 13. Measured pressure distribution along typical flow paths (feeding manifold - BUs - draining manifold) for $Ha = 1000$, $Re = 1000$.

5. Conclusions

The present paper gives a brief overview of liquid metal MHD activities performed at KIT in recent years in support of blanket engineering for a fusion DEMO reactor or for the ITER TBM. The work is based on a synergy between experimental and numerical analyses. Experiments have been carried out so far in the liquid metal facility MEKKA and provide data for fundamental problems in pressure-driven MHD duct flow and buoyant convection, in a parameter range relevant for applications in nuclear fusion. Results obtained from scaled mock-up experiments in entire columns of BUs may be used to validate blanket design concepts or to shed light on weak points of the design which require further optimization. The obtained experimental data serves for validation of theoretical work and numerical simulations that received particular interest in recent years due to the availability of high performance computing. The latter allows considering increasingly complex geometries and operating conditions typical in fusion reactors, in which large temperature gradients and intense magnetic fields are present. After full commissioning of MaPLE following its relocation from UCLA to KIT, a second complementary facility will be available for future MHD experiments using the prototypical liquid metal alloy PbLi.

The selected results discussed in this manuscript represent just a few examples to show the broad spectrum of MHD activities at KIT. Unfortunately, in this overview paper it is not possible to discuss all problems in full detail, but interested readers may find complete information in original papers to which we refer to.

CRedit authorship contribution statement

L. Bühler: Conceptualization, Data curation, Investigation, Project administration, Supervision, Validation, Writing – review & editing. **H.-J. Brinkmann:** Investigation, Resources. **C. Courtessole:** Data curation, Investigation, Writing – review & editing, Validation. **V. Klüber:** Data curation, Investigation, Software, Validation, Visualization. **C. Koehly:** Data curation, Investigation, Visualization. **B. Lyu:** Data curation, Investigation, Visualization. **C. Mistrangelo:** Data curation, Formal analysis, Investigation, Software, Validation, Visualization, Writing – review & editing. **J. Roth:** Investigation, Resources.

Declaration of competing interest

The authors declare that they have no known competing financial interests or personal relationships that could have appeared to influence the work reported in this paper.

Data availability

Data will be made available on request.

Acknowledgments

This work has been carried out within the framework of the EUROfusion Consortium, funded by the European Union via the Euratom Research and Training Programme (Grant Agreement No 101052200 – EUROfusion). Views and opinions expressed are however those of the author(s) only and do not necessarily reflect those of the European Union or the European Commission. Neither the European Union nor the European Commission can be held responsible for them.

References

- [1] M. Abdou, N.B. Morley, S. Smolentsev, A. Ying, S. Malang, A. Rowcliffe, M. Ulrickson, Blanket/first wall challenges and required R & D on the pathway to DEMO, *Fusion Eng. Des.* 100 (2015) 2–43, <http://dx.doi.org/10.1016/j.fusengdes.2015.07.021>.
- [2] C. Mistrangelo, L. Bühler, C. Koehly, I. Ricapito, Magnetohydrodynamic velocity and pressure drop in manifolds of a WCLL TBM, *Nucl. Fusion* 61 (2021) 096037, <http://dx.doi.org/10.1088/1741-4326/ac18dc>.
- [3] C. Mistrangelo, L. Bühler, C. Alberghi, S. Bassini, L. Candido, C. Courtessole, A. Tassone, F.R. Ugorri, O. Zikanov, MHD R & D activities for liquid metal blankets, *Energies* 14 (2021) 6640, <http://dx.doi.org/10.3390/en14206640>.
- [4] C. Mistrangelo, L. Bühler, V. Klüber, Towards the simulation of MHD flow in an entire WCLL blanket mock-up, *Fusion Eng. Des.* 193 (2023) 113752, <http://dx.doi.org/10.1016/j.fusengdes.2023.113752>.
- [5] V. Klüber, Three-Dimensional Magnetohydrodynamic Phenomena in Circular Pipe Flow (Ph.D. thesis), Karlsruhe Institute of Technology, 2023, <http://dx.doi.org/10.5445/IR/1000156159>.
- [6] L. Bühler, C. Mistrangelo, A simple MHD model for coupling poloidal manifolds to breeder units in liquid metal blankets, *Fusion Eng. Des.* 191 (2023) 113552, <http://dx.doi.org/10.1016/j.fusengdes.2023.113552>.
- [7] L. Bühler, C. Mistrangelo, Geometric optimization of electrically coupled liquid metal manifolds for WCLL blankets, in: *IEEE Transactions on Plasma Science* (2023) submitted Proceedings of IEEE Symposium on Fusion Engineering, SOFE, Oxford, 09-13 July, 2023, in press.
- [8] M.-J. Ni, R. Munipalli, N.B. Morley, P. Huang, M.A. Abdou, A current density conservative scheme for incompressible MHD flows at a low magnetic Reynolds number, Part I: on a rectangular collocated grid system, *J. Comput. Phys.* 227 (1) (2007) 174–204.
- [9] A.G. Kulikovskii, Flows of a conducting incompressible liquid in an arbitrary region with a strong magnetic field, *Fluid Dyn.* 8 (1) (1974) 462–467, Russian original (1973).
- [10] L. Bühler, Magnetohydrodynamic flows in arbitrary geometries in strong, nonuniform magnetic fields, *Fusion Technol.* 27 (1995) 3–24.
- [11] L. Bühler, G. Aiello, S. Bendotti, C. Koehly, C. Mistrangelo, J. Galabert, Development of combined temperature - electric potential sensors, *Fusion Eng. Des.* 136 (2018) 7–11, <http://dx.doi.org/10.1016/j.fusengdes.2017.12.004>.
- [12] L. Bühler, H.-J. Brinkmann, C. Koehly, Experimental study of liquid metal magnetohydrodynamic flows near gaps between flow channel inserts, *Fusion Eng. Des.* 146 (2019) 1399–1402, <http://dx.doi.org/10.1016/j.fusengdes.2018.11.034>.
- [13] L. Bühler, C. Mistrangelo, H.-J. Brinkmann, C. Koehly, Pressure distribution in MHD flows in an experimental test-section for a HCLL blanket, *Fusion Eng. Des.* 127 (2018) 168–172, <http://dx.doi.org/10.1016/j.fusengdes.2018.01.007>.
- [14] C. Mistrangelo, L. Bühler, Determination of multichannel MHD velocity profiles from wall-potential measurements and numerical simulations, *Fusion Eng. Des.* 130 (2018) 137–141, <http://dx.doi.org/10.1016/j.fusengdes.2018.03.041>.
- [15] C. Courtessole, H.-J. Brinkmann, L. Bühler, J. Roth, Experimental investigation of MHD flows in a WCLL TBM mock-up, *Fusion Eng. Des.* submitted, Proceedings of 15th International Symposium on Fusion Nuclear Technology, ISFNT-15, Las Palmas de Gran Canaria, Spain, 10-15, 2023.
- [16] L. Barleon, K.-J. Mack, R. Stieglitz, The MEKKA-Facility a Flexible Tool To Investigate MHD-Flow Phenomena, *Tech. Rep. FZKA 5821*, Forschungszentrum Karlsruhe, 1996.
- [17] S. Smolentsev, F.-C. Li, N. Morley, Y. Ueki, M. Abdou, T. Sketchley, Construction and initial operation of MHD PbLi facility at UCLA, *Fusion Eng. Des.* 88 (2013) 317–326, <http://dx.doi.org/10.1016/j.fusengdes.2013.03.018>.
- [18] C.B. Reed, B.F. Picologlou, T.Q. Hua, J.S. Walker, Alex results - A comparison of measurements from a round and a rectangular duct with 3-D code predictions, in: *12th Symposium on Fusion Engineering*, Monterey, California, October 13-16, IEEE, 1987, pp. 1267–1270.
- [19] B.F. Picologlou, C.B. Reed, Experimental investigation of 3-D MHD flows at high Hartmann number and interaction parameter, in: J. Lielpeteris, R. Moreau (Eds.), *Liquid Metal Magnetohydrodynamics*, Kluwer, Dordrecht, 1989, pp. 71–77.

- [20] X. Albets-Chico, D. Grigoriadis, E. Votyakov, S. Kassinos, Direct numerical simulation of turbulent liquid metal flow entering a magnetic field, *Fusion Eng. Des.* 88 (2013) 3108–3124, <http://dx.doi.org/10.1016/j.fusengdes.2013.09.002>.
- [21] S. Smolentsev, S. Badia, R. Bhattacharyay, L. Bühler, L. Chen, Q. Huang, H.-G. Jin, D. Krasnov, D.-W. Lee, E. Mas de les Valls, C. Mistrangelo, R. Munipalli, M.-J. Ni, D. Pashkevich, A. Patel, G. Pulugundla, P. Satyamurthy, A. Snegirev, V. Sviridov, P. Swain, T. Zhou, O. Zikanov, An approach to verification and validation of MHD codes for fusion applications, *Fusion Eng. Des.* 100 (2015) 65–72, <http://dx.doi.org/10.1016/j.fusengdes.2014.04.049>.
- [22] L. Bühler, H.-J. Brinkmann, C. Mistrangelo, Experimental investigation of liquid metal pipe flow in a strong non-uniform magnetic field, *Magneto-hydrodynamics* 56 (2020) 81–88, <http://dx.doi.org/10.22364/mhd.56.2-3.4>.
- [23] L. Bühler, B. Lyu, H.-J. Brinkmann, C. Mistrangelo, Reconstruction of 3D MHD liquid metal velocity from measurements of electric potential on the external surface of a thick-walled pipe, *Fusion Eng. Des.* 168 (2021) 112590, <http://dx.doi.org/10.1016/j.fusengdes.2021.112590>.
- [24] V. Klüber, C. Mistrangelo, L. Bühler, Numerical simulation of 3D magnetohydrodynamic liquid metal flow in a spatially varying solenoidal magnetic field, *Fusion Eng. Des.* 156 (2020) 111659, <http://dx.doi.org/10.1016/j.fusengdes.2020.111659>.
- [25] S. Malang, *Einrichtung zur Verringerung des MHD-Druckverlustes in dickwandigen Kanälen*, 1987, Patent DE 36 00 645 C2.
- [26] C. Koehly, L. Bühler, Fabrication issues of sandwich-like flow channel inserts for circular pipes, *Fusion Sci. Technol.* 72 (2017) 660–666, <http://dx.doi.org/10.1080/15361055.2017.1350477>.
- [27] L. Bühler, C. Mistrangelo, H.-J. Brinkmann, Experimental investigation of liquid metal MHD flow entering a flow channel insert, *Fusion Eng. Des.* 154 (2020) 111484, <http://dx.doi.org/10.1016/j.fusengdes.2020.111484>.
- [28] O. Zikanov, I. Belyaev, Y. Listratov, P. Frick, N. Razuvanov, V. Sviridov, Mixed convection in pipe and duct flows with strong magnetic fields, *Appl. Mech. Rev.* 73 (2021) 010801–1–35, <http://dx.doi.org/10.1115/1.4049833>.
- [29] U. Burr, U. Müller, Rayleigh-Bénard convection in liquid metal layers under the influence of a vertical magnetic field, *Phys. Fluids* 13 (11) (2001) 3247–3257.
- [30] U. Burr, L. Barleon, P. Jochmann, A. Tsinober, Magneto-hydrodynamic convection in a vertical slot with horizontal magnetic field, *J. Fluid Mech.* 475 (2003) 21–40.
- [31] C. Koehly, L. Bühler, C. Mistrangelo, Design of a test section to analyze magneto-convection effects in WCLL blankets, *Fusion Sci. Technol.* 75 (2019) 1010–1015, <http://dx.doi.org/10.1080/15361055.2019.1607705>.
- [32] C. Mistrangelo, L. Bühler, H.-J. Brinkmann, C. Courtessole, V. Klüber, C. Koehly, Magneto-convective flows around two differentially heated cylinders, *Heat Mass Transf.* 59 (2023) 2005–2021, <http://dx.doi.org/10.1007/s00231-023-03350-2>.
- [33] C. Courtessole, H.-J. Brinkmann, L. Bühler, Experimental investigation of magneto-convective flows around two differentially heated cylinders, *J. Fluid Mech.* (2023) in review.
- [34] C. Koehly, L. Bühler, C. Courtessole, Design of a scaled mock-up of the WCLL TBM for MHD experiments in liquid metal manifolds and breeder units, *Fusion Eng. Des.* 192 (2023) 113753, <http://dx.doi.org/10.1016/j.fusengdes.2023.113753>.